Post-print of: Pietrzak T., Gołębiewska A., Płachta J., Jarczewski M., Ryl J., Wasiucionek M., Garbarczyk J.: Photoluminescence of partially reduced Eu2+/Eu3+ active centers in a NaF–Al2O3–P2O5 glassy matrix with tunable smooth spectra. JOURNAL OF LUMINESCENCE. Vol. 208(2019), pp. 322-326. DOI: 10.1016/j.jlumin.2018.12.060

Photoluminescence of partially reduced Eu^{2+}/Eu^{3+} active centers in a $NaF–Al_2O_3–P_2O_5$ glassy matrix with tunable smooth spectra

Tomasz K. Pietrzak*[a], Agata Gołębiewska[a], Jakub Płachta[b], Michał Jarczewski[a], Jacek Ryl[c], Marek Wasiucionek[a], Jerzy E. Garbarczyk[a]

[a] *Faculty of Physics, Warsaw University of Technology, Koszykowa 75, 00-662 Warsaw, Poland*
[b] *Institute of Physics, Polish Academy of Sciences, Lotników 32/46, 02-668 Warsaw, Poland*
[c] *Faculty of Chemistry, Gdańsk University of Technology, Narutowicza 11/12, 80-233 Gdańsk, Poland*

Abstract

In this work, a series of photoluminescent materials have been synthesized based on optically transparent and chemically stable glasses of the nominal composition $Na_3Al_2(PO_4)_2F_3$ ($NaF–Al_2O_3–P_2O_5$ system) doped with 1 wt % of europium. It has been shown that the synthesis conditions (mainly the temperature and duration of the melting stage under reducing conditions) strongly affected the photoluminescence spectra of the material. This effect has been ascribed to varying proportions between Eu^{3+} and Eu^{2+} ions concentrations, imposed by the synthesis conditions, which was confirmed by XPS, absorption and decay times measurements. As both Eu^{3+} and Eu^{2+} centers exhibit photoluminescence in different ranges of the visible spectra (Eu^{3+} – red, and Eu^{2+} – mainly blue) the possibility, shown by us, to control relative proportions of the oxidation states of europium and consequently to control the photoluminescence spectra, may be advantageous from the viewpoint of potential applications of such materials as novel phosphors for white LEDs with the emission spectra resembling natural light.

Keywords: tunable luminescence; europium facile reduction; glassy matrix; scalable synthesis

1. Introduction

Lighting belongs to major global consumers of the electrical energy. For decades it has been dominated by energy-inefficient conventional incandescent, halogen or fluorescent lamps. Only in recent years we have witnessed a rapid replacement of those obsolete light sources by much more energy efficient solid state white light emitting diodes (LED). It is prognosed that due to the implementation of white LED lighting, the energy demand by lighting in USA alone will be reduced in 2035 by ca 60 percent compared to 2014, despite increased lighting capabilities [1]. An important advantage of white LEDs over conventional light sources, besides their efficiency, is their very long term of service (typically ca 25 000 hrs vs. 1 000 hrs for incandescent bulbs) [1]. One of serious shortcomings of early white LED light sources – their high cost – has already been substantially reduced, making them affordable for nearly any user. Unfortunately, one serious disadvantage of white LED technology still persists – the deviation of their emission spectra from those of the natural light. This shortcoming, common for most commercial white LEDs, has raised many concerns about negative effects of the white LED-based illumination on human vision, leading to eyes' fatigue and/or even to serious irreversible vision-related physiological changes (e.g. [2, 3]). One of the main directions to improve that situation consists in synthesizing new phosphor materials whose luminescence spectra would better resemble the natural light.

Nowadays, the most successful phosphor materials, in terms of similarity of their emission spectra to natural light, are based on solid matrices doped with photoluminescent centers, such as e.g. Eu^{2+}, Eu^{3+}, Dy^{3+}, Yb^{2+} and many others, (e.g. [4, 5, 6, 7, 8]). As numerous studies have shown, it is very important both to select the matrix material and the luminescent agents to achieve the goal, because the actual emission of given centers may strongly differ depending on the matrix. Among many materials successfully tested as matrices for europium-based phosphors there are many crystalline orthophosphates, including the ones with the NASICON structure [4].

Europium-doped phosphors are commonly used in white LEDs, because both Eu^{2+} and Eu^{3+} exhibit strong photoluminescence in the visible range [4]. The former ions emit light in the broad "cool" blue range due to $5d \rightarrow 4f$ transitions [9], while the latter ones exhibit narrow lines in a "warm" red (amaranth-tinted) range due to $4f \rightarrow 4f$ transitions [10]. From the viewpoint of applications it is very attractive to purposely adjust the emission spectra of the europium doped phosphors by modifying Eu^{2+}/Eu^{3+} relative concentrations. This can be done by various technological processes [11].

Members of our research group at Warsaw University of Technology have been working for years on many versatile glassy compounds that are promising materials for

*Corresponding author, tomasz.pietrzak@pw.edu.pl

cathodes in Na-ion / Li-ion batteries, including those with NASICON-type structure (e.g. $Na_3V_2(PO_4)_2F_3$ [12] or $Li_3V_2(PO_4)_2F_3$ [13]). From previous studies, members of our group have gained a lot of experience in synthesizing glasses containing transition metal oxides at different oxidation states, e.g. iron [14] (Fe^{2+}/Fe^{3+}) or vanadium [15] (V^{5+}/V^{4+}). In this paper, we propose a $Na_3Al_2(PO_4)_2F_3$ NASICON-related transparent glass doped with europium as novel phosphor for white LEDs. To the best of our knowledge, the only study on NaF–Al_2O_3–P_2O_5 glass was that by Pronklin et al. who focused mainly on electrical properties of the materials [16, 17]. The advantage of our proposal is the simple and cheap synthesis, as well as the possibility of adjusting the relative Eu^{2+}/Eu^{3+} ratio at an early stage of the molten batch before the glass quenching. Presumably, no studies in this direction have been reported in the literature.

Figure 1: A schematic view of a double crucible technique. The inner crucible contains the batch. The outer crucible is half-filled with activated charcoal and covered with a lid. At elevated temperatures activated charcoal bonds with oxygen creating CO, which is a reducing agent.

2. Experimental

The syntheses started from the melting of an appropriate mixture of initial reagents: NaF (Sigma-Aldrich, > 99 %), Al_2O_3 (POCh – Polish Chemicals, p.a.), $NH_4H_2PO_4$ (POCh, 99.5%) and Eu_2O_3 (POCh, 99.9 %) as a source of europium photoluminescence centers. Three batches with a fixed concentration of 1 wt% of dopant were melted at different temperature (1000–1350 ℃) and time (5–15 min), using a double crucible technique with the outer lidded crucible filled with charcoal (Fig. 1) [18]. Above 1000 ℃ the predominant product of burning charcoal in air is CO rather than CO_2 (due to so-called Boudouard reaction), which allows us to provide a reducing atmosphere to the sample during synthesis process. Eventually, the melts were rapidly cooled down to room temperature between two stainless-steel plates (melt-quenching technique). The parameters of the syntheses are listed in Tab. 1.

XRD measurements were carried out with a Philips X'Pert Pro diffractometer using the CuKα line ($\lambda = 1.542$ Å) to check amorphousness of the synthesized samples. Glass transition and crystallization temperatures were determined from DTA measurements carried out in argon flow in a TA Q600 apparatus with the heating rate of 10 ℃/min.

In order to quantitatively determine the relative concentration of Eu^{2+}/Eu^{3+} luminescence centers, high-resolution X-ray photoelectron spectroscopy (XPS) studies were carried out at Gdańsk University of Technology on an Escalab 250 Xi from Thermofisher Scientific. The spectroscope was equipped with $Al_{K\alpha}$ source. Pass energy was 30 eV and the spot size diameter was 250 mm. Charge compensation was controlled through the low-energy electron and low energy Ar^+ ions emission by means of a flood gun (emission current 150 mA, beam voltage 2.1 V, filament current 3.5 A), with normalization of the X-axis (binding energy) for the peak characteristics of neutral carbon C 1s (284.6 eV) [19, 20]. Avantage software (Thermofisher Scientific) was used for deconvolution purposes.

All of the optical characterizations were conducted at the Institute of Physics at Polish Academy of Sciences. For photoluminescence measurements (PL), a He-Cd laser with $\lambda = 325$ nm was used as a source of excitation. PL spectra at room temperature were acquired in 350–750 nm range using an Andor Shamrock SR-303i-B spectrometer equipped with Andor iDus CCD camera. A filter was chosen accordingly to the laser wavelength in order to cut out the laser line. The samples were fixed onto a black plate with double sided adhesive carbon tape (black).

For the time-resolved photoluminescence the samples were excited by a pulsed laser at 375 nm at room temperature. The laser was triggered by an external generator at 20 kHz. Signal from the sample was then analyzed and correlated using a Pico Harp 300 photon counting system and an Excelitas AQRH photon counting module equipped with an avalanche diode. The lifetimes were measured at two distinct wavelengths – one characteristic for Eu^{3+} transition and one for the Eu^{2+} transition, i.e 611 nm and 510 nm, respectively.

The absorption measurements were performed at room temperature using a Varian Cary 50 UV-Vis Spectrophotometer equipped with Xenon lamp as a source and silicon diode detector. The samples were attached to designated holders using a cyanoacrylate glue. Neither the holders nor the glue contributed significantly to the absorption spectrum; the spectrum from the holder was used as a baseline and was subtracted from the results.

3. Results and discussion

DTA traces were typical for glasses (Fig. 2) and consisted of a glass transition (ca. 420 ℃) followed by a crys-

Table 1: Parameters of the syntheses.

Label	Melting time	Melting temperature
A	5 mins	1100 ℃
B	10 mins	1300 ℃
C	15 mins	1350 ℃

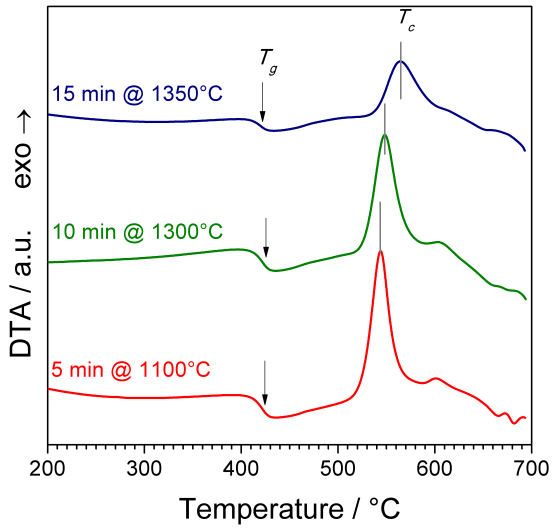

Figure 2: DTA scans of as-synthesized glassy samples measured with heating rate of 10 ℃/min in argon flow.

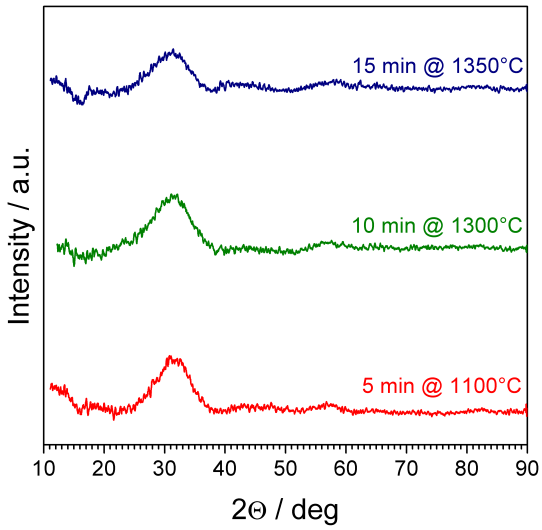

Figure 3: XRD patterns of as-synthesized glassy samples.

tallization peak. The crystallization temperatures (544–564 ℃) were higher for samples with longer melting time. Such correlation was observed by us also in case of another, significantly different glass composition: $90V_2O_5 \cdot 10P_2O_5$ [21]. This DTA experiment showed that the matrix was thermally stable to at least 400 ℃, which is a fairly sufficient range for typical applications.

XRD patterns (Fig. 3) of the samples were in agreement with DTA results, i.e. they were typical for glassy materials. They consisted of a characteristic amorphous halo, and no crystalline peaks were visible.

Fig. 4 shows the comparison of high-resolution XPS spectra registered in the Eu3d energy range, for each investigated material. The spectra are divided into two groups of peaks, namely Eu3$d^{5/2}$ and Eu3$d^{3/2}$, shifted approx. 30 eV. The relatively low intensity recorded derivates from low amount of europium in the glass samples. The fitting procedure was carried out using Gaussian-Lorentzian functions. The Eu3$d^{5/2}$ spectra are composed of two primary peak doublets located at 1124.4 and 1134.6 eV, further ascribed to Eu^{2+} and Eu^{3+} states respectively. The deconvolution revealed different relative intensity for each sample, while the peak positions were in a very good agreement with other XPS studies [22, 23, 24, 25]. The Eu^{2+}/Eu^{3+} ratio was then estimated on the base of peak doublets analysis and summarized in Tab. 2. However, one should be aware that XPS is a surface method. Therefore the share of Eu^{3+} ions determined from this spectroscopy may be overestimated due to oxidation processes at the surface of the samples. Nevertheless, it can be seen that growing temperature and time of synthesis resulted in better partial reduction of Eu^{3+} to Eu^{2+}.

As expected, the synthesis conditions had a strong influence on the photoluminescence spectra (Fig. 5a-c). The effective color of emission varied from amaranth (5 min at 1100 ℃), through "warm" white (10 min at 1300 ℃) to "cool" white (15 min at 1350 ℃). This phenomenon is due to different relative concentration of Eu^{3+} and Eu^{2+}.

The spectra were deconvoluted with *Fityk* 0.9.8 software [26] using Gaussian profiles. In general, two types of lines were observed: narrow and wide ones. Narrow lines above 575 nm were identified as 4f – 4f transitions in Eu^{3+}. The values of the positions and full width at half maximum (FWHM) are presented in Tab. 3. They were evident in samples A and B, whereas in sample C only one weak narrow line at 611.3 nm was detectable (as shown in inset in Fig. 5c). Below 600 nm, broad emission lines of Eu^{2+} were observed. It was difficult to non-ambiguously fit Gaussian profiles to collected data in this range. Nevertheless, all data sets contain broad peak centered at 506–521 nm, which probably can be ascribed to $4f^6 5d^1 \rightarrow {}^8S_{7/2}$ transition in Eu^{2+}.

In Fig. 7, decay curves of the studied samples for $\lambda_{em} =$ 510 nm are shown. The best fit was achieved for $N = 3$

Table 2: The share of europium oxidation states, based on high-resolution XPS analysis.

Label	Eu^{2+}	Eu^{3+}
A	33 %	67 %
B	36 %	64 %
C	42 %	58 %

Table 3: Comparison of positions (λ) and FWHM of emission lines of Eu^{3+} centers observed in the studied samples A–C. All values are given in nanometers. Optical transitions were ascribed according to Refs. [27] and [28]. Slightly different wavelengths ascribed to the same optical transition are due to Stark splitting.

Transition	λ_A	λ_B	λ_C	$FWHM_A$	$FWHM_B$	$FWHM_C$
$^5D_0 \rightarrow ^7F_0$	578.3	578.2	—	2.2	6.7	—
$^5D_0 \rightarrow ^7F_1$	589.0	586.9	—	8.0	7.2	—
$^5D_0 \rightarrow ^7F_1$	595.6	594.2	—	7.0	12.9	—
$^5D_0 \rightarrow ^7F_2$	611.7	611.5	611.3	4.0	3.9	—
$^5D_0 \rightarrow ^7F_2$	617.2	616.3	—	11.5	12.9	—
$^5D_0 \rightarrow ^7F_3$	652.9	—	—	8.3	—	—
$^5D_0 \rightarrow ^7F_4$	693.1	693.8	—	12.5	16.8	—
$^5D_0 \rightarrow ^7F_4$	701.7	701.8	—	7.9	7.7	—

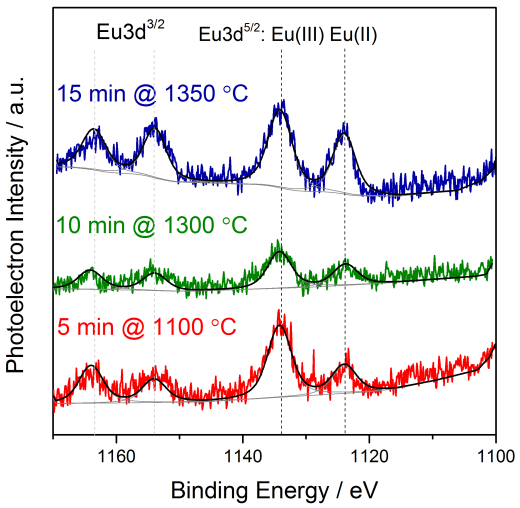

Figure 4: The Eu3*d* high-resolution XPS spectra of investigated samples.

decay times, i.e. according to formula:

$$I(t) = \sum_{i=1}^{N} A_i \exp\left(-t/\tau_i\right) \quad (1)$$

The fitting parameters are shown w Tab. 4. The corresponding decay times are with the same order of magnitude in each samples. However, a systematic increase in the values is observable with the growing temperature/time of the synthesis. These results are in a good agreement with decay times reported for Eu^{2+} $5d \rightarrow 4f$ transitions [29]. Similar experiment was repeated for $\lambda_{em} = 611$ nm. In this case, no measurable decay was observed withing 32 μs from the excitation, which was the maximum observation time in the experimental setup. Such long decay times are characteristic for Eu^{3+} $4f \rightarrow 4f$ forbidden transitions [30]. Thus, one can conclude that the wide emission at low wavelengths should be ascribed to presence of Eu^{2+} active centers, whereas narrow lines at higher wavelengths are due to Eu^{3+} ions.

Absorption spectra of samples A and B are shown in Fig. 8. Two sharp absorption lines are evident in case of sample A: 395 and 465 nm. According to Ref. [31], these can be attributed to $^7F_0 \rightarrow ^5L_6$ and $^7F_0 \rightarrow ^5D_2$ transitions in Eu^{3+}, respectively. In case of sample B, where concentration of Eu^{3+} is lower and Eu^{2+} higher, only a smooth absorption edge at ca 425 nm was observed. Such spectra were reported for samples containing Eu^{2+} [32]. It was verified that none of these phenomena is related to a pure matrix (i.e. without Eu doping).

To conclude, XPS, photoluminescence, decay time and absorption measurements have proved that higher time and temperature of syntheses resulted in partial reduction of Eu^{3+} to Eu^{2+}. Eu^{3+} exhibits narrow absorption lines and high lifetime, whereas Eu^{2+} shows broad absorption and low lifetime.

4. Conclusions

The most pronounced outcome of this work is that our not complicated route of the synthesis resulted in smooth, continuous PL spectra with tunable white color. Similar spectra are barely reported in the literature and demand sophisticated synthesis routines (e.g. [33]).

The study has shown that by controlling synthesis parameters (i.e. time and temperature) in a reducing atmosphere one can tune up a desirable effective color of photoluminescence in studied samples. In case of aliovalent Eu^{2+}/Eu^{3+} ions, it was possible to tune the color from amaranth through warm white to cool white. Furthermore, relatively smooth spectra of some of the synthe-

Table 4: Decay times obtained from curves in Fig. 7.

Label	A_1	τ_1 / ns	A_2	τ_2 / ns	A_3	τ_3 / ns
A	0.754(1)	4.95(2)	0.221(1)	61.9(3)	0.081(3)	714(2)
B	0.747(2)	4.68(2)	0.242(1)	63.4(3)	0.092(1)	734(3)
C	0.396(2)	15.1(1)	0.277(1)	184(1)	0.266(1)	1085(2)

sized samples are advantageous for applications, because they resemble continuous spectra of the natural light and should provide good color rendering. The exact values of the color rendering index (CRI) and the luminous efficacy will be measured in the next stage of our studies.

In this research we decided to use a $NaF–Al_2O_3–P_2O_5$ matrix, with composition similar to cathode materials for electrochemical cells previously studied by us. Lack of ions that may exist at different oxidation levels was its important advantage, accompanied by inexpensive precursors and scalable route of synthesis. Nonetheless, we believe that the tuning of Eu^{2+}/Eu^{3+} ratio to obtain white phosphors with smooth spectra may be achieved in other glassy matrices with mechanical, chemical and optical properties chosen accordingly to any desired applications.

Acknowledgments

We are thankful to Ms. Anna Borodziuk, M.Sc. (Institute of Physics, PAS) for help in absorption measurements. The authors wish to acknowledge Ms. Aleksandra Stawczyk, a former B.Sc. student of T.K. Pietrzak, who also contributed to this research.

References

References

[1] P. Morgan Pattison, M. Hansen, J.Y. Tsao, Comptes Rendus Phys. 19 (2018) 134–145.
[2] F. Viénot, P. Mottier (Ed.), LEDs Light. Appl., ISTE Ltd., (2009) 197–232.
[3] E. Chamorro, C. Bonnin-Arias, M.J. Pérez-Carrasco, J.M. De Luna, D. Vázquez, C. Sánchez-Ramos, Photochemistry and Photobiology 89 (2013) 468–473.
[4] K.N. Shinde, S.J. Dhoble, Crit. Rev. Solid State Mater. Sci. 39 (2014) 459–479.
[5] X. Lu, H. Liu, X. Yang, Y. Tian, X. Gao, L. Han, Q. Xu, Ceram. Int. 43 (2017) 11686–11691.
[6] S. Ye, F. Xiao, Y.X. Pan, Y.Y. Ma, Q.Y. Zhang, Mater. Sci. Eng. R Reports. 71 (2010) 1–34.
[7] Z. Xia, Z. Xu, M. Chen, Q. Liu, Dalt. Trans. 45 (2016) 11214–11232.
[8] J. Liu, A.M. Kaczmarek, R. Van Deun, Chem. Soc. Rev. 47 (2018) 7225–7238.
[9] D. Dutczak, T. Jüstel, C. Ronda and A. Meijerink, Phys. Chem. Chem. Phys. 17 (2015) 15236–15249.
[10] K. Binnemans, Coordination Chemistry Reviews 295 (2015) 1–45.
[11] S. Ghosh, Sh. Bhaktha, Nanotechnology 29 (2018) 225202.
[12] I.L. Matts, St. Dacek, T.K. Pietrzak, R. Malik, G. Ceder, Chemistry of Materials 27 (2015) 6008–6015.
[13] T.K. Pietrzak, P.P. Michalski, M. Wasiucionek, J.E. Garbarczyk, Solid State Ionics 288 (2016) 193–198.
[14] T.K. Pietrzak, P.P. Michalski, P.E. Kruk, W. Ślubowska, K. Szlachta, P. Duda, J.L. Nowiński, M. Wasiucionek, J.E. Garbarczyk, Solid State Ionics 302 (2017) 45–48.
[15] T.K. Pietrzak, W.K. Zajkowska, M. Wasiucionek, J.E. Garbarczyk, Solid State Ionics 322 (2018) 11–17.
[16] G.I. Evstrop'eva, I.A. Sokolov, Yu.P. Tarlakov, V.N. Naraev, A.A. Pronkin, Glass Physics and Chemistry 24 (1998) 561–568.
[17] I.A. Sokolov, V.N. Naraev, A.A. Pronkin, Glass Physics and Chemistry 26 (2000) 588–593.
[18] K. Hirose, T. Honma, Y. Benino, T. Komatsu, Solid State Ionics 178 (2007) 801–807.
[19] K. Siuzdak, M. Szkoda, A. Lisowska-Oleksiak, J. Karczewski, J. Ryl, RSC Adv. 6 (2016) 33101–33110.
[20] J. Wysocka, S. Krakowiak, J. Ryl, Electrochimica Acta 258 (2017) 1463–1475.
[21] T.K. Pietrzak, J.E. Garbarczyk, M. Wasiucionek, J.L. Nowiński, Physics and Chemistry of Glasses: European Journal of Glass Science and Technology Part B 57 (2016) 113–124.
[22] S. Kumar, R. Prakash, R.J.Choudhary, D.M.Phase, Materials Research Bulletin 70 (2015) 392–396.
[23] L.A. Zavala-Sanchez, G.A. Hirata, E. Novitskaya, K. Karandikar, M. Herrera, O.A. Graeve, ACS Biomater. Sci. Eng. 1 (2015) 1306–1313.
[24] H.C. Swart, I.M. Nagpure, O.M. Ntwaeaborwa, G.L. Fisher, J.J. Terblans, Optics Express 20 (2012) 17119–17125.
[25] Z. Haque, G.S. Thakur, R. Parthasarathy, B. Gerke, Th. Block, L. Heletta, R. Pöttgen, A.G. Joshi, G.K. Selvan, S. Arumugam, L.Ch. Gupta, A.K. Ganguli, Inorg. Chem. 56 (2017) 3182–3189.
[26] M. Wojdyr, J. Appl. Cryst. 43 (2010) 1126–1128.
[27] G. Gao, N. Da, S. Reibstein, L. Wondraczek, Optics Express 18 (2010) A575–583.
[28] W.A. Pisarski, L. Żur, J. Pisarska, Optics Letters 36 (2011) 990–992.
[29] N. Guo, Y. Jia, W. Lü, W. Lv, Q. Zhao, M. Jiao, B. Shao, H. You, Dalton Transactions 42 (2013) 5649–5654.
[30] Sh. Qi, Y. Huang, T. Tsuboi, W. Huang, H.J. Seo, Optical Materials Express 4 (2014) 396–402.
[31] S. Balaji, P.A. Azeem, R.R. Reddy, Physica B 394 (2007) 62–68.
[32] P. Dai, Sz.-P. Lee, T.-Sh. Chan, Ch.-H. Huang, Y.-W. Chiang, T.-M. Chen, Mater. Chem. C 4 (2016) 1170–1177.
[33] F. Wang, Y.-h. Chen, C.-y. Liu, D.-g. Ma, Chem. Commun. 47 (2011) 3502–3504.

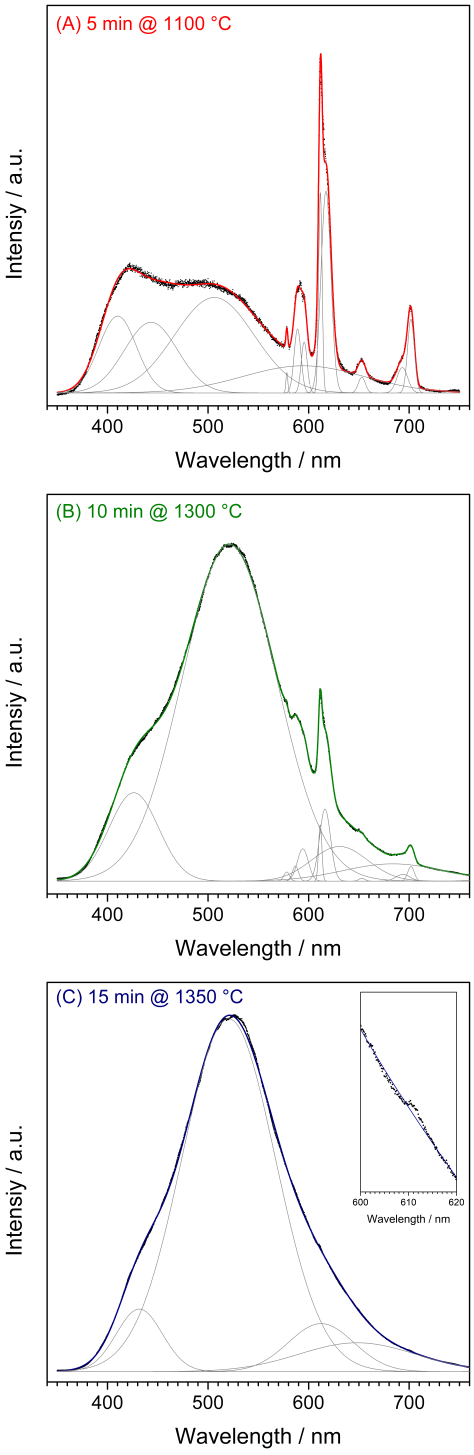

Figure 5: Photoluminescence spectra of the studied samples synthesized under different conditions. $\lambda_{ex} = 325$ nm. Deconvolution curves are included.

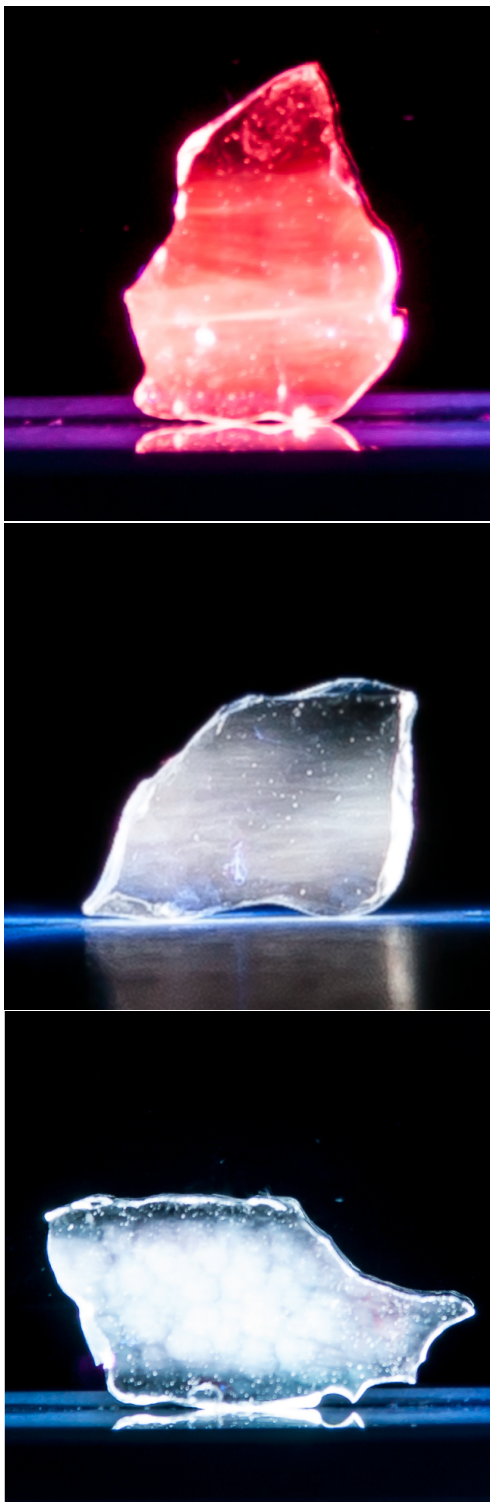

Figure 6: Photographs of photoluminescence of samples A (top), B (middle) and C (bottom) excited by a blue laser diode. The samples are ca. 1 cm high.

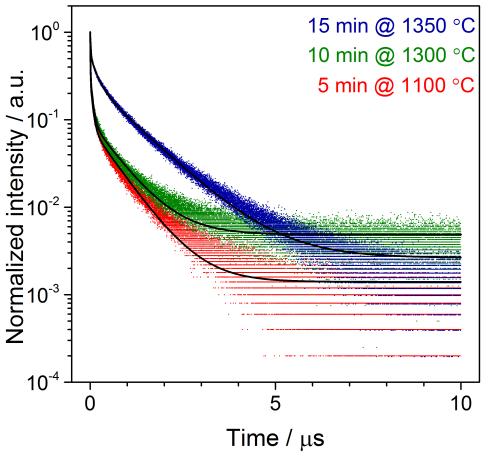

Figure 7: Decay curves of three studies samples for $\lambda_{em} = 510$ nm. Black lines represent fits according to Eq. 1 with parameters listed in Tab. 4.

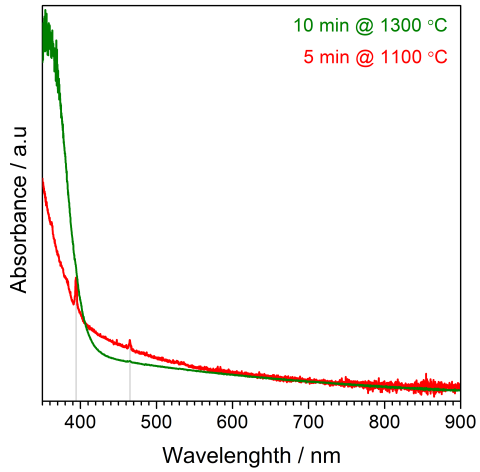

Figure 8: Absorption spectra of samples A and B.